Dependence of impurity transport on ρ^*, ν^*, rotation and MHD in NSTX

L. Delgado-Aparicio[1], D. Stutman[2], K. Tritz[2], F. Volpe[3], K. L. Wong[1], S. Gerhardt[1], E. Fredrickson[1], R. Bell[1], B. Leblanc[1], S. Kaye[1], J. Menard[1], M. Finkenthal[2], S. Paul[1] and L. Roquemore[1]

[1]Princeton Plasma Physics Laboratory, Princeton, NJ 08543-0451, USA (ldelgado@pppl.gov)
[2]Department of Physics and Astronomy, The Johns Hopkins University, Baltimore, MD 21218, USA
[3]Dept. of Engineering Physics, Wisconsin University, Madison, WI, 53706, USA

Abstract

An assessment of low-Z impurity transport have been performed using scans of $\rho*$ at constant q-profile and $\nu*$ at constant plasma density and toroidal field. Impurity diffusivity levels consistent with the neoclassical predictions have been found, whereas a reversal of the convective velocity at low fields indicates an anomalous effect to be at play at the gradient region. Studies of the impact of rotation in these H-modes show that heavy and not fully stripped impurities can experience diffusive and convective transport coefficients several times larger than that of the '*standard*' neoclassical transport for stationary plasmas, without the need of invoking the presence of long wavelength core electrostatic turbulence. As a by-product of a strong impurity accumulation we have also observed a correlation between the appearance of tearing mode activity and the strength of the emitted radiation posibly indicating a cooling mechanism within the magnetic island.

I. Motivation

The National Spherical Torus eXperiment (NSTX) [1] is a low-aspect ratio tokamak (A<1.5) that is able to sustain a high plasma β operating with B_ϕ~0.35-0.55 T, I_p~0.7-1.1 MA and a neutral beam (NBI) heating power up to 7.0 MW; the latter leads to core toroidal velocities of the order of 100-300 km/s and E×B shearing rates up to ~1 MHz. This shearing rate can be up to a factor of three to five greater than typical linear growth rates of long-wavelength ion temperature-gradient modes, suppressing these instabilities partially if not completely. One of the ST predicted benefits is therefore the reduction of the anomalous ion transport, resulting in low core (r/a<0.7) particle diffusivities in good agreement with the values predicted by neoclassical transport theory and important for the development of high confinement H-mode plasmas. Particle and impurity transport properties at low-aspect-ratio remain important for extrapolation to future ST-based devices such as an NSTX-Upgrade, NHTX and CTF [2] as well as to conventional aspect ratio schemes such as ITER. This paper is organized as follows: a description of the $\rho*\sim1/B^2$ and $\nu*\sim1/T^2$ scans of impurity transport in NBI heated H-modes is outlined in Section II; in Section III we discuss the the relationship between the enhanced particle fluxes and toroidal rotation, while a correlation between the strength of the emitted radiation, the plasma cooling and the appearance of tearing modes activity is discussed in Section IV.

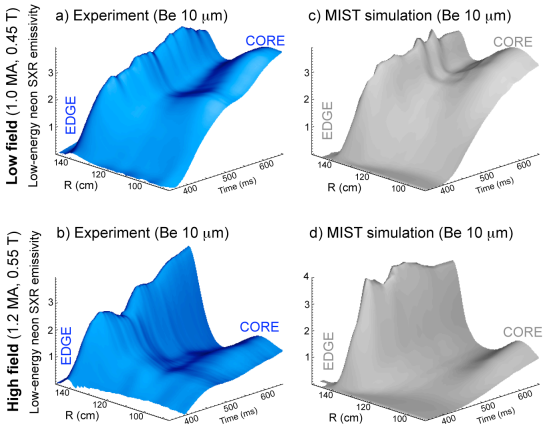

Fig. 1 Experimental and MIST simulated neon SXR emissivity profiles for low-field and high-field H-modes.

II. ρ^* and ν^* scans of impurity transport.

The first ρ^* impurity transport scaling experiments performed in beam-heated NSTX H-modes were done by simultaneously varying the external toroidal field and the plasma current to observe transport and confinement effects at fixed q_{95} [3]-[4]. The neon injection and

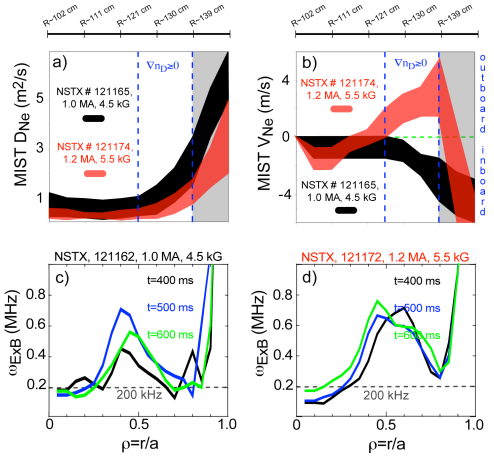

Fig. 2 MIST neon a) diffusion and b) convective velocity profiles together with that of E×B shear profiles for low and high field cases.

resultant impurity transport measurements were performed under two different conditions: the low-field (I_p=1.0 MA, B_ϕ=0.45 T) vs. the high-field (I_p=1.2 MA, B_ϕ=0.55 T) plasmas. Figures 1-a) and -b) depict the 2 ms time-averaged experimental neon SXR emissivities for both the low- and high-field cases [3]-[4]. A comparison between the edge and core signals in Figures 1 indicate that the impurity build-up and its subsequent penetration to the core have been changed substantially when both the plasma current and the toroidal field were increased as part of the fixed *q*-profile ion gyro-radius scan [4]. The time histories of the SXR neon emissivity profiles after the injection were modeled using the one-dimensional Multiple Ionization Stage Transport (MIST) code [5] [see Figures 1-c) and -d)]. Impurity diffusivity levels consistent with the neoclassical predictions have been found, whereas a reversal of the convective velocity in the low field case indicates some anomalous effect to be at play at the gradient region [see Figures 2-a) and –b)]. Tentatively, we attribute the needed (anomalous) negative pinch velocity at low fields, to the incomplete shear suppression of drift-wave-like instabilities [4] at an outer radii (r/a~0.7-0.8) [see Figure 2-c) and compare with wider E×B shear rates at high field]; experimental findings of neoclassical diffusivity with anomalous convective velocity have also been reported in high aspect ratio tokamaks (see [4], [8] and references therein).

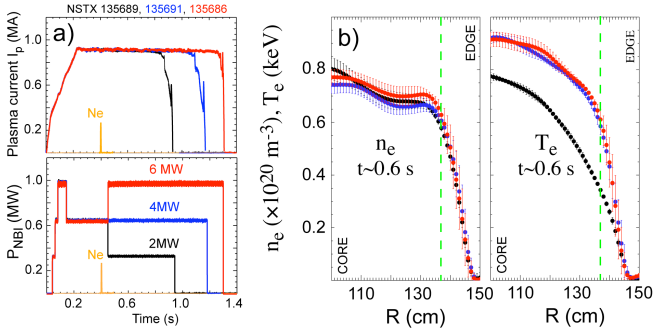

Fig. 3 ν* scan varying NBI power.

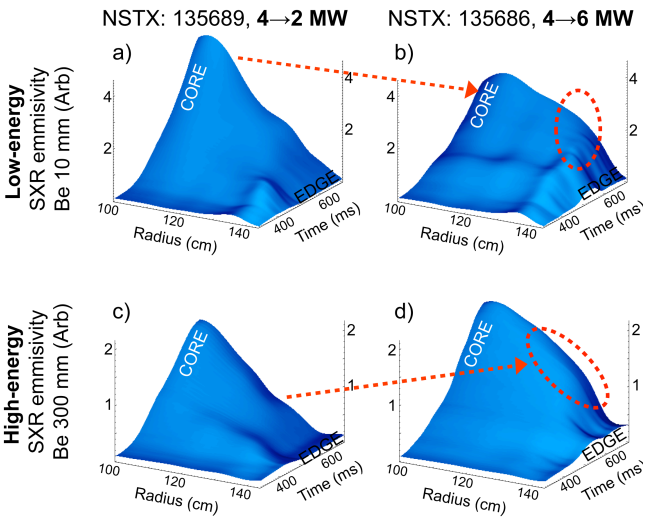

Fig. 4 Low- and high-energy emissivities for the 2 and 6 MWcases.

A ν^*-scan of impurity transport was designed to complement the observations at low fields described above, but this time, using distinct NBI heated plasmas with n, I_p and B_ϕ held constant (see Figure 3); the high-power discharges have as much as twice the ion and electron temperatures in the gradient region [see Figure 3-b), r/a~0.6-0.8] relative to that at low power, with an associated ν^* varying up to a factor of four with nearly identical density profiles. Low- and high-energy SXR emissivity reconstructions for the 2 and 6 MW cases are shown for comparison in Figure 4. The low-energy emissivities sensitive to line radiation from He- and H-like Neon ions indicate that the core emissivity decreases with NBI power while increasing at mid-radius. However, the high-energy emissivity suggest that both the core and mid radius

signals increases with NBI power indicating a possible change in the transport characteristics at the gradient region where ν^* was varied. Preliminary results from MIST simulations [see Figure 5] indicate however, that a factor of two increases in T_e (0.6<r/a<0.8) could be solely responsible for modifying the neon charge state distribution and thus the SXR emissivity. In summary, different charge state distributions as a consequence of different background plasma parameters have to be taken into account when modeling the impurity transport, and may be responsible of the observation of a change in emissivity in the ν^* scan experiments, without the need of changing the underlying transport.

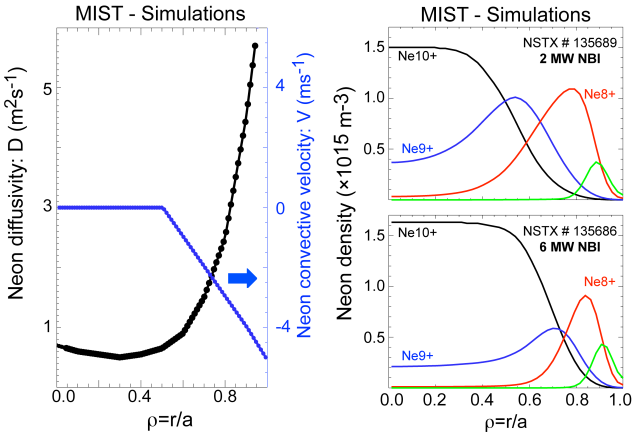

Fig. 5 MIST diffusion and convective transport coefficients together with the different density of neon charge states for the 2 and 6 MWcases.

III. Enhanced Pfirsch-Schlüter impurity flux in the core of a rotating plasma.

The time-independent impurity transport studies described above have used traces of neon gas-puffs into a MHD-free phase of well established H-mode discharges; these plasmas were characterized by a constant increase in the core electron density due to central NBI fueling and impurity accumulation, that translated in a continuous decrease in the core toroidal velocity. The motivation for performing impurity transport experiments using impurity-embedded pellets is to assess the time-dependent characteristics of the transport matrix by probing the time evolving effects of quantities such as toroidal rotation. In addition, it is pertinent to the NSTX and NSTX-Upgrade research and development to find a reliable model to extrapolate the transport characteristics at high toroidal velocities in low-density H-mode scenarios since the '*standard*' neoclassical theory [6] derived for low Mach numbers may not be applicable [7]. A first experimental assessment [9] was done using a 0.5 mg ablation-resistant vitreous carbon pellet deposited at mid-radius. The evolution of the perturbed impurity density δn_Z is considerably slower than that of cold pusle (δT_e) and thus estimates of carbon diffusivity can be obtained using the 1D-radial transport code MIST [see Figure 6]. While the carbon diffusivity in the outward plasma (r/a>0.6) seem to agree well with neoclassical ordering of ~1 m^2/s as described above, the core transport appears to be enhanced above the neoclassical values reaching several times the NCLASS predictions (5-7 m^2/s) [9]. The effect of plasma rotation on transport has been considered as the best '*non-turbulent*' candidate to explain this enhanced diffusivity since high centrifugal forces could account for the enhancement of heat and particle transport over the stationary, or so-called, standard neoclassical theory.

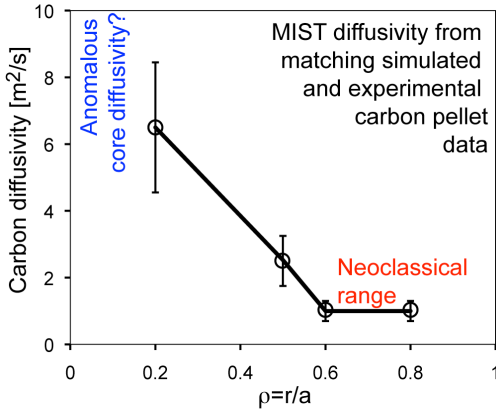

Fig. 6 MIST carbon diffusion for the early phase of an NSTX H-mode [9].

Motivated by the contradictory results from several tokamaks such the ISX-B [10], PLT [11] and JET [12], as well as existing theories that predict that impurity transport can be altered by

an external momentum source, Wong *et al.* [13]-[14] and Romanelli *et al.* [15]-[16] investigated impurity particle orbits to predict a modified Pfirsch-Schlüter transport in the frame of a rotating plasma. Though appear to be qualitatively different, it has been determined that is possible to re-write the equations derived by Wong and Romanelli using the same functional form as described in equation (1), were M_D is the deuterium Mach number and "γ" depends on the impurity mass, charge and the T_i/T_e ratio [17]. In a stationary plasma (Ω=0), these two models reduce to the charge independent Pfirsch-Schlüter impurity diffusivity; moreover, this enhanced particle diffusivity depends on even powers of "Ω" and thus is independent of the direction of plasma rotation, explaining some of the results from PLT using co- and counter-propagating beams [10].

$$D_Z^{PS}(\Omega) = D_Z^{PS}(\Omega = 0)\left[1 + \gamma \cdot M_D\right]^2 \qquad (1)$$

$$M_D \approx 1.05 \times 10^{-5} v_\phi^2[\mathrm{km/s}]/T_D[\mathrm{keV}] \qquad (2)$$

$$\gamma = \frac{A}{2}\left\{1 - \frac{2Z}{A}\left(\frac{T_e}{T_e + T_i}\right)\right\} \qquad (3)$$

The mass-, charge- and temperature-dependence of "γ" are shown in Figures 7-a) and -b) for different impurities from carbon to molybdenum. The effect of having a higher T_i/T_e ratio is equivalent to "reduce" the impurity charge (Z) which in turn will result in increasing "γ" [see equation (3)]; impurities which are not fully-stripped (e.g. neon-like argon and iron) may have ~20% higher "γ"s which can translate also into higher diffusivities. Synthetic data describing peaked ion-temperatures of 1.0 keV and a normalized toroidal velocity have been generated using Lorentzian profiles; the resultant deuterium Mach numbers have been computed for the cases of core velocities of 100, 200 and 300 km/s and are shown in Figure 7-c). An intermediate case of modified Pfirsch-Schlüter diffusivities (using a core v_ϕ~200 km/s) for fully stripped and He-like carbon and neon are compared with the "non-rotating" counterpart [see Figure 7-d)]. This comparison shows good agreement at the outer radii since Mach numbers are low (M_D<0.1), but a rather large discrepancy at the core where the enhancement takes place (M_D>0.1). The theoretical result for carbon diffusivity appears to be in accordance with the experimental result shown above. The change of impurity diffusivity is even more dramatic if one considers the mass-dependence at a constant impurity charge as shown in Figure 7-e); the fully stripped neon and the neon-like argon or iron can have an enhanced diffusivity as much as one to two-orders of magnitude higher than its "non-rotating" neoclassical counterpart. In summary, the collisional Pfirsch-Schlüter neoclassical diffusivity for heavy impurities can be one to two orders of magnitude higher in a deuterated rotating plasma than in a stationary one, without the need of invoking the presence of long

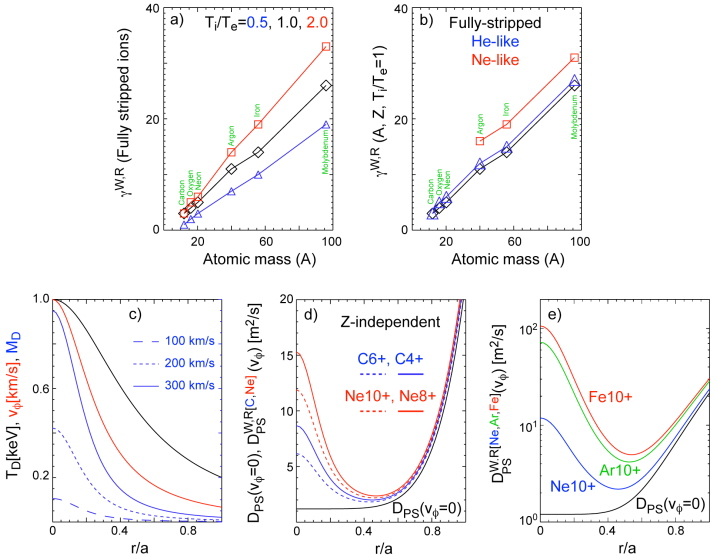

Fig. 7 a) Temperature-, b) charge-state and mass-dependence of "γ". Synthetic profiles for ion temperature, normalized toroidal velocity and the resultant Mach numbers are indicated in c), while with the Pfirsch-Schlüter diffusivities for fully stripped and He-like carbon and neon are depicted in d). Enhanced diffusivities for fully stripped neon and neon-like argon and iron are shown in e).

wavelength electrostatic turbulence. Though the impurity peaking factors do not change from the standard neoclassical description, the enhanced diffusivity and convective velocity can account for an enhancement of the conventional Pfirsch-Schlüter impurity fluxes that could result in unexpected radiated powers.

IV. Radiation induced tearing modes.

The present study was motivated by the observation of the early appearance of tearing mode (TM) activity in neon-seeded H-modes in both the $\rho*$ (see Figure 3 in ref. [4]) and $\nu*$ scaling experiments described above. By the end of the current flattop for the discharges shown in Figure 3, we observed the development of a m/n=2/1 tearing mode as indicated also in Figure 8-a) [w/o neon injection]. The appearance of the tearing mode activity ~100 ms earlier in the neon-seeded H-mode appear to be related to the ~220 kW of enhanced radiated power from the neon emission; both the plasma density and temperatures profiles as well as total radiated power are similar before the two TM onsets. According to Figure 8-b), there is a sudden drop in the mid-radius high-energy (temperature-sensitive) SXR emissivity that correlates well in time with the increase of B_θ, as well as the asymmetric "inward" growth of the region with a 'flat' low-energy emissivity shown in the surface and normalized contour plots in Figure 8-c); the decrease of the low-energy emissivity for r/a<0.5 might also suggest a decrease in T_e(R,t) during the island growth. The multi-point Thomson scattering electron density and temperature profiles (not shown here) are in agreement with these qualitative statements for the first 50 ms from the mode-onset. The use of the multi-energy SXR diagnostic [4] allows us for the first time to simultaneously image both the effect of the island growth and cooling at mid-radius.

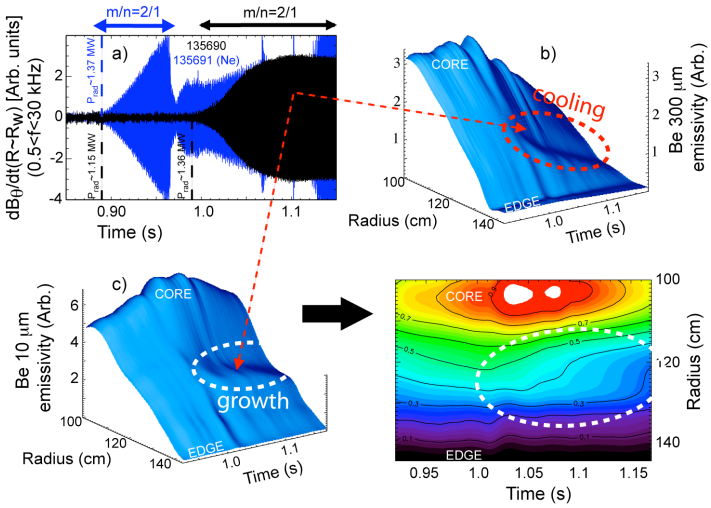

Fig. 8 a) Mirnov (dB/dt) data indicating the presence an MHD mode in H-mode plasmas with and without neon seeding. Both the cooling and growth of the island at mid-radius are observed using the b) high- and c) low-energy SXR emission.

Recent observations of exponentially-growing tearing modes in ASDEX-UPGRADE [18], RTP [19]-[21] and TEXTOR [22] tokamaks support the idea of having a driving mechanism proportional to the island size and the radiated power density which can be modeled using the extended Rutherford formalism used to describe Neo-classical Tearing Modes (NTMs) [23-25]; to avoid confusion with the NTM description and its driving mechanisms, Salzedas *et al.*, have coined the term Radiative induced Tearing Modes (RTM). The study of RTMs in present tokamaks is important for extrapolation to ITER since the presence of impurities in the edge and core of advanced ITER scenarios is guaranteed both by the edge radiation mantles and the radiation from heavy non-fully-stripped impurities used for diagnostic purposes. Therefore, verifying the linear scaling law between island growth rate and the island-size (ω) and radiated power from continuum and line emission ($P_{rad}=P_{cont}+P_{line}$) is important, as it predicts that an ST-based reactor and even ITER can be susceptible to TM destabilization by impurity radiation, and that TM control techniques must be implemented.

Dedicated TM scaling experiments have made use of different impurity amounts by extending the neon puff lengths, indicating a relationship between the strength of the radiation emitted, the appearance of the m/n=2/1 tearing mode as well as the island size; Figure 9 depicts the effect that a 10-50 ms Ne-puff have in anticipating the mode-onset by 20-80 ms in comparison to that without Ne injection. Both the electron density and temperature profiles before and during the mode onset for the neon-free and neon seeded H-modes are shown in Figure 10 and indicate good reproducibility in matching the conditions for the Δ' drive; the inserts are a "zoom" of the region of interest where the tearing mode develops. The time-history of the kinetic profiles appears to have at least qualitatively, the same behavior: the core electron density (temperature) increases (decreases) while both the density and temperature flattens at mid-radius. Quantitatively though, the electron temperature drops 130 eV in the neon-free case, indicating also a mid-plane island width of approximately 6 cm [see insert in Figure 10-c)], while in the neon-seeded plasma the electron temperature drop is of the order of 200 eV and a temperature-flattening extends across a length of ~9 cm. The change in electron pressure represents the energy loss per unit volume in the electron channel, henceforth, the estimated power losses (for a Δt~50 ms), indicate a effective cooling rate of approximately ~39.52 and ~97.8 mW/cm^3, respectively. Figure 11 illustrates the radiated power density [mW/cm^3] profiles measured by a tangential bolometer for both the neon-free and neon-seeded H-modes; the vertical dotted-line 'pin-points' the position where the tearing mode develops while the two horizontal lines indicate the first 50 ms from the mode onset. The radiated power density losses of 25 and 50 mW/cm^3 confirm the apparent relationship between the presence of the enhanced radiation, the strength of the cooling and the change in the extension of the temperature flattening.

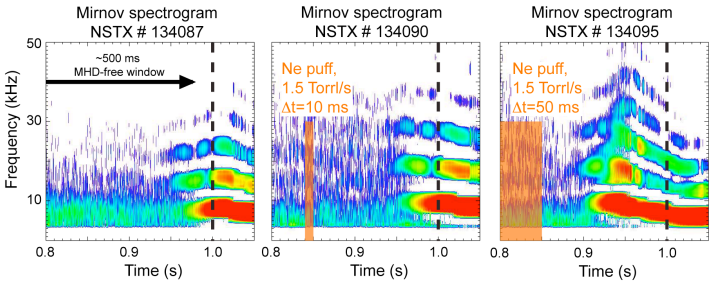

Fig. 9 Mirnov spectrograms indicating the effect of how the 10-50 ms Ne-puffs anticipate the mode onset by 20-80 ms.

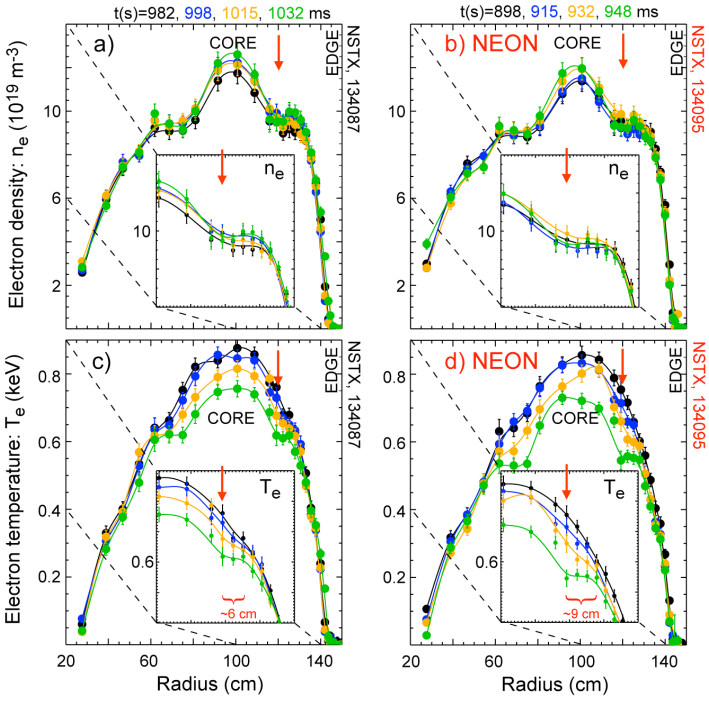

Fig. 10 Multi-point Thomson Scattering electron density and temperature data for NSTX shots 134087 and 134095 (neon-seeded). The inserts are a "zoom" of the region of interest where the tearing mode develops.

In addition, Figure 12 depicts the low- and high-energy SXR reconstructions for the neon-free and neon seeded H-modes discussed above. For the first, both the growth of the region with "flat" low-energy emissivity as well as the decrease in the high-energy emisivity indicating the plasma cooling are observed at late times in accordance with magnetics, the

bolometer and MPTS. For the neon-seeded case, it becomes clear that the slowly-increasing enhanced radiation from neon continuum and line-emission precedes the island formation in the region of interest [see Fugure 12-c)]. Moreover, the high energy emissivity also indicates that the plasma cooling at mid-radius took place after the impurity pile-up. In summary, we have found a correlation between the local enhanced neon-radiation, the early appearance of the mode onset at the location where the local radiation is increasing, the enhanced cooling rates as well as the increased island size given by the extension of the temperature-flattening. Furthermore, the enhancement of the high-energy emissivity is only of about 25% since it accounts for the increase of Z_{eff} due to a small impurity strength factor; the latter is also an estimate of how small is the increase in resistivity and thus the effect on Δ'. However, the enhancement of the low energy emissivity and thus of P_{line}, if of about 200-300% due to the strong He- and H-like emission, thus dominating over the incremental change given by resistivity and Bremsstrahlung (P_{cont}).

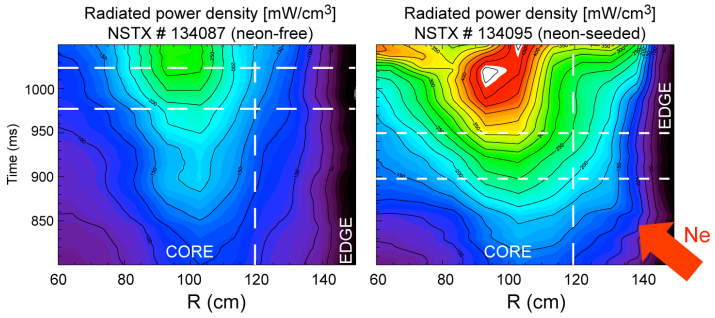

Fig. 11 Radiated power density profiles for the neon-free and neon-seeded H-mode before the tearing mode onset.

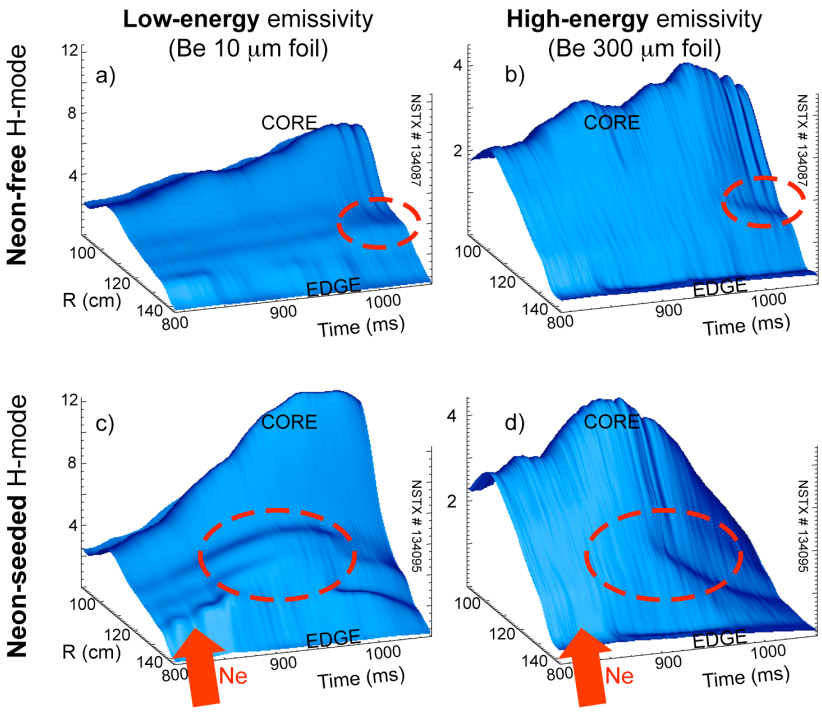

Fig. 12 Mirnov spectrograms indicating the effect of how the 10-50 ms Ne-puffs anticipate the mode onset by 20-80 ms.

V. Summary

An assessment of low-Z impurity transport have been performed using scans of $\rho*$ at constant q-profile and $\nu*$ at constant plasma density and toroidal field. Impurity diffusivity levels consistent with the neoclassical predictions have been found, whereas a reversal of the convective velocity at low fields indicates an anomalous effect to be at play at the gradient region. Different charge state distributions as a consequence of different background plasma parameters have been taken into account when modeling the impurity transport, and may be responsible of the observation of a change in emissivity in the $\nu*$ scan experiments, without the need of changing the underlying transport. Studies on the impact of rotation in low density H-modes show that heavy and not fully stripped impurities can experience diffusive and convective coefficients several times larger than that of the '*standard*' neoclassical transport for stationary plasmas without the need of invoking the presence of long wavelength core electrostatic turbulence. As a by-product of a strong impurity accumulation we have also observed a correlation between the strength of the emitted radiation, the plasma

cooling rates and the appearance of tearing modes activity. This work was supported by U.S. DoE Contract No. DE-AC02-09CH11466 at PPPL and DoE grant No. DE-FG02-99ER5452 at Johns Hopkins University.

References.

[1] M. Ono, *et al*., 2000, Nucl. Fusion, **40**, 557.
[2] Y-K. M. Peng, *et al*., 2005, Plasma Phys. Control. Fusion, **47**, B263.
[3] L. Delgado-Aparicio, *et al*., Plasma Phys. Controlled Fusion, **49**, 1245, (2007).
[4] L. Delgado-Aparicio, *et al*., Nucl. Fusion, **49**, 080528, (2009).
[5] R. Hulse, 1983, Nucl. Technol. Fusion, **3**, 259.
[6] W. Houlberg, *et al*., 1997, Phys. Plasmas, **4**, 3320.
[7] W. Houlberg, private communication, (2010).
[8] R. Guirlet, *et al*., 2006, Plasma Phys. Control. Fusion, **48**, B63.
[9] D. Stutman, et al., 33rd EPS Conference on Plasma Phys. Rome, 19 - 23 June 2006 ECA Vol.**30I**, P-5.120 (2006).
[10] R. C. Isler, *et al*.,, Phys. Rev. Lett., **47**, 649, (1981).
[11] S. Suckewer, *et al*., Nucl. Fusion, **24**, 815, (1984).
[12] B. Alper., *et al*., Proc. 23rd EPS Conf. on Plasma Physics and Controlled Fusion (Kiev, Ukraine, 24-28 June 1996) vol 1 (Geneva: EPS), p 163.
[13] K. L. Wong, *et al*., Phys. Rev. Lett., **59**, 2643, (1987).
[14] K. L. Wong, *et al*., Phys. Fluids B, **1**, 545, (1989).
[15] M. Romanelli, *et al*., Joint European Torus report \# JET-CP(98)31.
[16] M. Romanelli, *et al*., Plasma Phys. Control. Fusion, **40**, 1767, (1998).
[17] L. Delgado-Aparicio, *et al*., to be submitted to Nucl. Fusion, (2010).
[18] M. Schittenhelm, *et al*.,, Nucl. Fusion, **37**, 1255, (1997).
[19] A. A. M. Oomenes, *et al*., Exp3/09 paper, Proceeding of the 18th IAEA Fusion Energy Conference, Sorrento, October, 4-10, (2000).
[20] F. Salzedas, *et al*., 27th EPS Conference on Contr. Fusion and Plasma Phys. Budapest, 12-16 June 2000, ECA Vol. **24B** (2000) 25-28.
[21] F. Salzedas, *et al*., Phys. Rev. Lett., **88**, 075002-1, (2002).
[22] V.S. Udintsev, *et al*., Nucl. Fusion, **43**, 1424, (2003).
[23] P. H. Rutherford, PPPL Report 2277, (1985).
[24] E. Fredrickson, et al., Phys. Plasmas, **7**, 4112, (2000).
[25] E. Fredrickson, et al., Phys. Plasmas, **9**, 548, (2002).